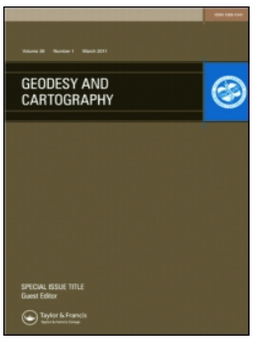

Geodesy and Cartography

ISSN: 2029-6991 (Print) 2029-7009 (Online) Journal homepage: http://www.tandfonline.com/loi/tgac20

Digital zenith camera of the University of Latvia

Ansis Zariņš, Augusts Rubans & Gunārs Silabriedis

To cite this article: Ansis Zariņš, Augusts Rubans & Gunārs Silabriedis (2016) Digital zenith camera of the University of Latvia, Geodesy and Cartography, 42:4, 129-135

To link to this article: http://dx.doi.org/10.3846/20296991.2016.1268434

Published online: 20 Dec 2016.

GEODESY AND CARTOGRAPHY
ISSN 2029-6991 / eISSN 2029-7009
2016 VOLUME 42(4): 129–135
https://doi.org/10.3846/20296991.2016.1268434

Taylor & Francis
Taylor & Francis Group

UDK 528.225

DIGITAL ZENITH CAMERA OF THE UNIVERSITY OF LATVIA

Ansis ZARIŅŠ, Augusts RUBANS, Gunārs SILABRIEDIS

Institute of Geodesy and Geoinformatics, the University of Latvia, Raiņa bulvāris 19, LV-1586 Rīga, Latvia
E-mails: ansiszx@inbox.lv (corresponding author); augusts.rubans@lu.lv; gunars.silabriedis@lu.lv

Received 29 November 2016; accepted 30 November 2016

Abstract. Design of digital zenith camera in Institute of Geodesy and Geoinformatics of the University of Latvia started in 2009. Now, after tests of a prototype, improvements of design and manufacturing of the second version, it has reached operational status. The paper describes construction of camera, features of it's control software. Vertical deflection determination results are discussed.

Keywords: zenith camera, GNSS coordinates, geodetic astronomy, vertical deflections, plumb line, geoid.

Introduction

Design of digital zenith camera in Institute of Geodesy and Geoinformatics of the University of Latvia started in 2010 (Abele *et al.* 2012). A simple prototype camera, employing manual rotation and leveling mechanisms, was constructed. Tests of it demonstrated necessity of computer control over most functional activities. Improvements of camera design included motorized rotation, leveling and focusing mechanisms. In order to simplify communication between the control computer and multiple actuators and data acquisition devices, an on-board control computer was added to the layout. The improved design (Fig. 1) was finished in 2015, extensive field tests were carried out in 2016. Presently, although some technical aspects still need improvements, we consider the camera ready for regular observations.

1. Camera design

Like other digital zenith cameras (Hirt 2004; Hirt *et al.* 2010; Tian *et al.* 2014), our design consists of a rotating platform, on it are mounted a small telescope, equipped with imaging device (CCD assembly), tiltmeter, leveling mechanism, rotation gear and control equipment. Similar platform below is used as base of leveling and rotation; it is mounted on a field tripod (Fig. 1). The CCD camera is attached in direct focus, below the telescope. The weight of rotating assembly is about 12 kg; it is easily detachable from tripod with the lower platform, and is transported in a separate case. The total weight of device and it's accessories is less than 30 kg.

The camera needs 12v / 3A power supply, it can be either a mains adapter or a battery (possibly, on-board).

1.1. Imaging system

A 8″ (203 mm) catadioptric telescope equipped with CCD camera is used for image acquisition. The camera has 8 Mpix sensor with 4.5 μm pixels; at 2 m focus distance resulting field of view is 0.5×0.39 dg with

Fig. 1. Zenith camera. All measuring devices and actuators are on the rotating upper platform

resolution close to 0.5″/pixel. We found that for zenith camera purposes 2×2 pixel binning mode (with resolution close to 1″/pixel) is advantageous due to increase of sensitivity and decrease of image file size and download time. Besides, bigger pixels lessen tendency of image fragmentation, caused by air turbulence effects. Loss of image details at decreased resolution only slightly affects resulting coordinate accuracy.

Exposure duration of 0.3–0.5 sec proved to be optimal. Image elongation becomes pronounced for longer exposures; shorter exposures result in smaller number of stars and in some loss of accuracy – while star position residual dispersion in a frame is a bit smaller for shorter exposures, estimated zenith position dispersion increases, probably due to lesser extent of averaging of air turbulence effects.

At above exposure settings, images of stars up to 13.5–14 magnitude are automatically recognized (Fig. 2). That ensures typically 10 to 100 stars per frame; frames with less than 10 stars occasionally can occur only when imaged area is far from galactic plane. Details of recognition and identification of star images are provided in (Zariņš *et al.* 2014).

1.2. Exposure timing and site coordinates

An on-board GNSS receiver is used for site coordinate acquisition and exposure moment determination. Receiver's event timing mechanism is used to obtain accurate moments of CCD shutter open/close events. Control PC's time is synchronized with GNSS receiver's 1 PPS signal with a few millisecond accuracy before start of data acquisition session on a site. After that, PC time of exposure request can be used for shutter event recognition and also as a backup for exposure moment determination if event mechanism fails. Site GNSS coordinates are saved in session information file and in a sites database record. Although coordinate accuracy, provided by on-board GNSS receiver, is quite adequate, coordinates can be adjusted at post-processing if more reliable data is available.

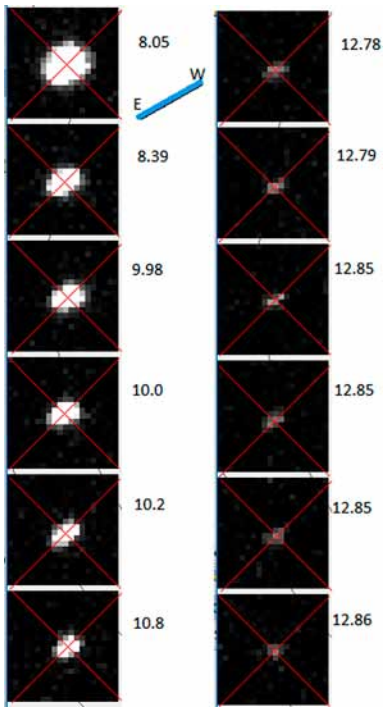

Fig. 2. Star images in a frame (close to Milky Way, 0.5 sec exposure, 2×2 pixel binning). Left: 6 brightest stars; right: weaker stars (#40-46 of 78). East – West direction outlined

1.3. Leveling and residual tilt determination

In each measurement position zenith camera assembly is leveled with a few arc second accuracy, using on-board tiltmeter as reference. Besides, the tiltmeter readings are registered during measurement session and used in data post-processing for residual tilt compensation.

A two-channel tiltmeter (Kahlmann *et al.* 2004) is installed on the zenith camera. It has very high resolution (a fraction of milliarcsecond) in a limited (±2 arcminutes) tilt range. The tiltmeter is interfaced via RS-232 connection and can provide up to 10 measurements per second. Leveling is done by stepper motor driven linear actuators, mounted on the edge of the rotating platform. They can lift the rotating platform up from the base platform for about 12 mm in ~0.01 μm (~0.02″ tilt) increments. The whole leveling process takes 10–20 seconds, depending on initial tilt and microseismics level. The main speed-limiting factor is mechanical oscillations, induced by actuator movements, the next leveling move can be calculated only when tiltmeter readings are reasonably calmed down, typically about 0.5 sec after the previous correction. The achievable leveling accuracy can not be better than combined microseismics and post-move oscillations amplitude; a practical limit was found to be about 1–1.5″. Besides, there is no much use of more accurate leveling because during measurement sessions erratic tilt changes are present, especially if tripod is placed on ground (Fig. 3). Placement on solid (paved) surfaces somewhat improves situation. Typical tilt change amplitude of a few arc seconds and period of a few minutes was observed, speed of tilt changes were up to hundreds of arc seconds per hour (Figs 3, 4). Linear approximation of dependency of tilt on time within frame data acquisition interval (Fig. 4) can be used to compensate the effect (at least, partially).

An on-board multi-channel stepper motor controller with full microstepping capability is used to

control actuator and mount rotation motors. Controller also includes digital I/O facility, used for actuator end-switches, PC time synchronization and other functions.

1.4. Rotation mechanism

When leveling actuators are retracted, the rotating platform assembly rests on three small wheels and can be rotated by any angle. Presently a stepper motor with a friction wheel directly on axis is used as rotation drive. Alternatively, a timing belt around lower platform and a pulley on a stepper motor axis is being considered for this purpose, for friction wheel performs poorly in freezing conditions. Rotation uses standard ramp acceleration/deceleration feature, offered by motor controller. Rotation speed of up to ~5 rpm is used, so rotation for 180 dg takes about 10 seconds.

In normal conditions friction mechanism ensures 1–3% relative accuracy of rotation angle. We find that quite acceptable, for high accuracy of rotation angle is not a critical parameter. Actual frame orientation, found within astrometric post-procession of frame data with one arcminute or better accuracy, is used in calculation of final results.

1.5. Control software

On-board computer running Windows is used for data acquisition control. Control and data processing software is designed as a single program, it can run either in measurement or post-processing modes. Difference between modes is mainly in data acquisition hardware treatment. On-board control process is monitored and controlled on a remote console (a laptop) via Remote-Desktop connection.

All hardware components except CCD communicates with control software via RS-232 connections. As control computer does not have adequate number of built-in RS-232 ports, USB-hosted RS-232 adapters are used. A timer-activated control loop is implemented in control program, regularly performing query on active devices. If new data is present, it is read, interpreted and visualized, any necessary actions are executed or scheduled. In case of time-consuming high priority operations (such as CCD image read-out) control loop can stop for quite long time (up to several seconds), so precautions are taken to avoid undesirable consequences.

Although in principle data processing and vertical deflection calculation can be done in real time, we found such mode time-consuming and not practical.

Fig. 3. Erratic tilt changes within 100 seconds. Tripod on unpaved ground

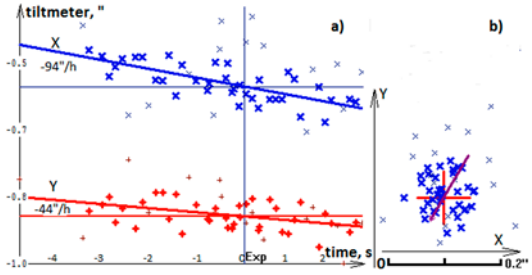

Fig. 4. Tiltmeter readings during frame exposure: a) dependence on time; b) in tiltmeter coordinate system. Approximating linear trend outlined. Outlying (thin) points were removed from analysis

Generally, measurement data are saved in file system and processed later. Exceptions are some critical data quality indicators, such as tiltmeter data dispersion and quality of star images on CCD image, which always are calculated in real time.

A number of control parameters, involved in measurement process, are stored in software configuration file and can be adjusted by operator.

In order to automate measurement process, session scenario mechanism is used. A scenario is a list of measurement position descriptors, including rotation angle before the position and number of frames in that position. It permits to perform all necessary measurements practically without operator intervention. On the other hand, a fully manual operation mode is also supported, allowing to execute wide variety of experimental measurements.

2. Observation procedure

Technically, the device can be deployed by a single person. The procedure starts with planting and leveling the field tripod. Leveling accuracy is not very critical, 0.1–0.2 dg is sufficient. An electronic or bubble level is used to control tripod leg length adjustment. After that, the rotating assembly is inserted on top of tripod, it is switched on, remote desktop connection is established, control software is started and data acquisition can begin.

Instrument was designed with intention to make it deployable wherever a tripod can be firmly placed. Test results indicate, that there are some drawbacks in using soft ground – amplitude of erratic movements

is bigger, walking or other activities in a few meters vicinity of the device affects tilt, so precautions must be taken. Also, nearness of buildings, heat sources, objects, prone to reflect GNSS signals, are undesirable.

Sequence of observation positions and number of frames taken in each position is determined by scenario specifications. Presently it seems, that most representative information can be obtained using 5–8 equally spaced rotation positions (with rotation for 50–80 dg in between), taking 10–20 frames in each position. Also, 180 dg rotation, interposed after each few positions with 90 or 60 dg rotation to obtain representation of more orientations, seems promising. At rotation plus leveling time of up to one minute and frame data acquisition time of about 8 seconds, one position takes about 3 minutes. Presently, in the sake of data redundancy, 2 full rotations usually are performed in each direction, that takes altogether about one hour. In the future, the scenario probably will be simplified, making session duration shorter.

Frame data acquisition begins with tiltmeter data quality check – only if dispersion of last 5–10 readings are within tolerance limit, frame can proceed with collecting a requested number of tiltmeter readings, then CCD exposure and additional tiltmeter readings. CCD image is immediately analyzed, if 6 or more star images are found, the frame is accepted. Position is concluded when requested number of accepted frames are present; in the absence of star images up to twice the requested number of frame attempts are made.

In order to limit effect of erratic tilt changes, releveling is executed if at the start of a frame tiltmeter position has drifted too far from zero point.

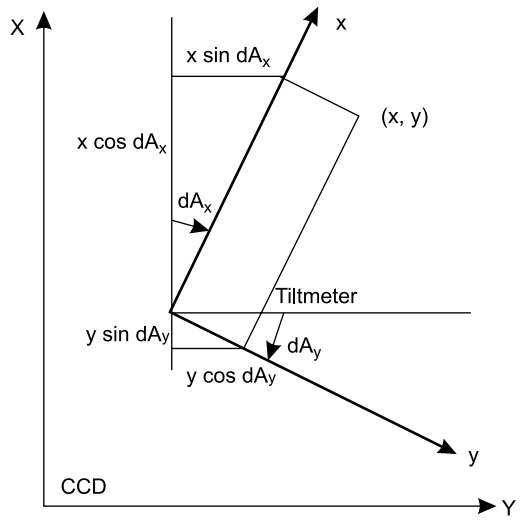

Fig. 5. Transformation of tiltmeter readings to CCD coordinate system

3. Data model

Our approach to obtaining vertical deflection values from observation data is somewhat different from generally seen for zenith cameras (Hirt 2004; Hirt *et al.* 2010; Tian *et al.* 2014), it might be called an instrumental one. We believe that in comparison to traditional calculation of astronomical coordinates of site and then finding vertical deflection as difference from ellipsoidal (geodetic) coordinates, it offers more transparent interpretation of measurements and simpler procedure of calculation. The approach is based on analysis of the pattern, made by calculated reference ellipsoid normal's projections on CCD coordinate system when instrument is rotated. These projections are obtained for each frame, iteratively calculating position on frame for a (imaginary) star with apparent place in zenith. If the instrument would be ideally leveled (in the sense of closeness to tiltmeter zero) in each rotation position, plumb line would project in a single point in CCD coordinate system (with location, determined by tiltmeter zero-point offsets and tiltmeter orientation relative to imaging subsystem). Trajectory of reference ellipsoid's normal would be a circle around plumb line's projection (Abele *et al.* 2012). Parameters of this circle (radius and phase) would give components of vertical deflection value.

In reality, leveling can never be ideal, therefore corrections, obtained from tiltmeter measurements during frame exposure, must be applied to calculated reference ellipsoid normal's projection coordinates. Calculation of these corrections is somewhat complicated by the fact, that it is technically difficult to accomplish perfect alignment of tiltmeter and CCD axes, so misalignment values must be taken into account. Assuming that CCD axes are perpendicular to each other, and both CCD and tiltmeter's planes are close to perpendicular to plumb line, correction values are determined by two orientation angles dAx and dAy between CCD and tiltmeter X and Y axes respectively (Fig. 5):

$$\begin{aligned} dX &= x \cdot Sx \cdot \cos(dAx) - y \cdot Sy \cdot \sin(dAy), \\ dY &= x \cdot Sx \cdot \sin(dAx) + y \cdot Sy \cdot \cos(dAy), \end{aligned} \qquad (1)$$

where *dX, dY* – corrections to projection coordinates, *Sx, Sy* – scale factors of tiltmeter axes; *x, y* – tiltmeter readings. Constant offsets are omitted in (1), for they affect only position of trajectory, not shape and size.

A special observation scenario was devised for measurements of tiltmeter orientation angles *dAx*, *dAy* and scale factors *Sx*, *Sy*. It is performed in a fixed rotation position and consists of series of frames, tilting platform in such a way, that one of tiltmeter channels

keeps it's value unchanged as much, as possible. Calculation of appropriate tilting actuator movements is based on geometry of actuator and tiltmeter configuration. At about 200 arc seconds tilt range, linearity of tilt trajectory within 0.1–0.2 arc seconds can be ensured. Resulting ellipsoidal zenith positions in CCD coordinate system and tilt positions in tiltmeter coordinate system both make almost linear trajectories. Comparing both trajectories, angles between relevant axes of CCD and tiltmeter can be found. Measurements must be performed separately for X and Y axes.

Calculation of tiltmeter trajectory orientation involve conversion of tiltmeter readings to physical units (e.g., arc seconds). Described angle measurement scenario allows also for determination of scale factors, used in this conversion. If orientation of CCD and tiltmeter axes are close to parallel or perpendicular, scale factors can be calculated simply comparing distance, traveled by zenith on CCD image to the corresponding change in tilt value. In case of arbitrary orientation, all involved parameters – orientation angles and scale values – must be calculated in a complex way.

Accuracy of such angle and scale factor determination is limited by properties of involved instrument subsystems. The prevailing factor seems to be astrometric zenith point accuracy on CCD – typically it has star position residual rms value between 0.3 and 0.5 arc seconds. The second biggest contribution is tiltmeter measurement dispersion. It depends on microseismics level and erratic drift properties, in good conditions it is 0.03–0.1 arc seconds. As a result, relative scale accuracy of up to 0.25% and orientation angle accuracy of up to 0.1 dg can be reached.

The above procedure of tiltmeter scale and orientation determination functionally closely resembles calibration procedure, described in (Hirt *et al.* 2010; Hirt 2004).

According to (1), impact of axes orientation and scale factor errors on measured zenith position corrections is proportional to value of tiltmeter readings and, consequently, to leveling accuracy. Therefore, accurate leveling in each rotation position is important. However, erratic tilt changes (Fig. 3) make too accurate leveling useless, for it very soon deteriorates. Therefore 1–2 arc seconds seems to be an optimal leveling accuracy threshold value. At tiltmeter readings within a few arc second range, impact of orientation angle and scale uncertainties do not exceed 0.01–0.02 arc seconds and is noticeably below impact of fluctuations in atmosphere, microseismics, other incidental factors.

Additional effect, complicating calculation of vertical deflection values, is thermal expansion in mechanical construction of device, changing relative orientation of tiltmeter and imaging system. Possibly, there is also drift of tiltmeter zero-points, which cannot be distinguished from thermal expansion effects. Analysis of results indicate, that summary relative orientation drift is quite noticeable and has typical value of several arc seconds per hour. Although course of this drift can be complex and include erratic components with tens of minutes to hours typical period, a considerable part of it can be approximated by linear time trend in corrected zenith positions and added to session data model. Because of averaging of erratic component, short duration (a few minutes) approximating models show much bigger drift values (and better approximation accuracy) than long-duration (tens of minutes or more) models.

4. Observation results

A number of test observation sessions at a fixed site were carried out in order to find actual capabilities of device and select optimal observation methodology. It was found, that, in most aspects, performance is close to expected. Properties of some subsystem performance are already discussed above.

Impact of a number of factors, determining accuracy of the final result – components of vertical deflection – can be demonstrated analysing behaviour of static mode observations, when device's position is not changed. An example of results of such session is provided on Figure 6. Due to erratic tilt changes, thermal deformations of construction elements, changes in atmosphere conditions, possibly, other reasons, position of calculated place of reference ellipsoid normal's projection on CCD image (Fig. 6a) and tiltmeter's readings (Fig. 6b) are changing in time both in systematic and in random ways. Amplitude of these changes typically is about several arc seconds; speed of systematic component – several arc seconds per hour. Substantial part of changes is identical in both subsystems, reflecting changes in orientation of whole device (tripod). In the corrected zenith position, calculated according (1), this part is removed, resulting in much smaller amplitude of remaining changes (Fig. 6c). They represent sum of a number of incidental impacts (turbulence of atmosphere, randomly shifting images of stars, microseismics, reference star catalog errors, irregular part of thermal deformations) and also a systematic trend, reflecting slow changes in relative orientation of

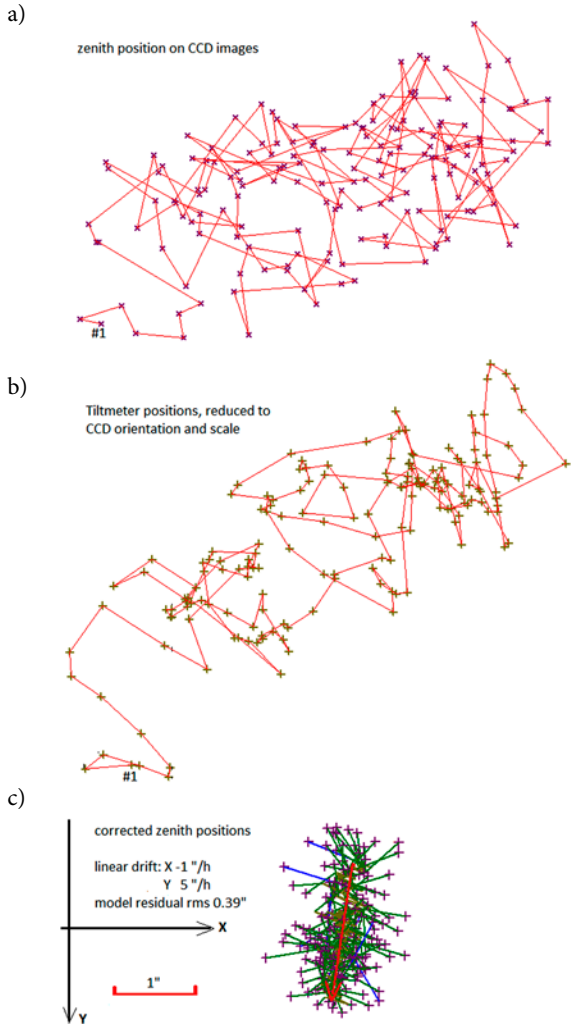

Fig. 6. Static observation session: a) ellipsoidal zenith, b) tiltmeter, c) corrected zenith positions. Consecutive frames connected in a) and b). Model approximation residuals for corrected positions outlined in c)

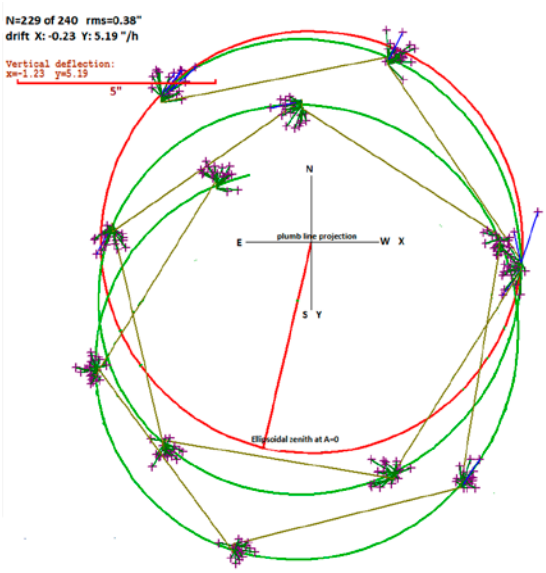

Fig. 7. Observation session results. Corrected frame zenith positions in CCD coordinate system, approximated by a circle, linearly moving in time. Vertical deflection value outlined in topocentric system (view upwards)

both subsystems due to thermal deformations, drift of tiltmeter zero points and, possibly, other effects. After applying linear approximating model, the remaining residuals are mostly incidental and have rms value typically within interval from 0.25 to 0.5 arc seconds. For long duration observation sessions linear model fits increasingly worse, it seems to be a critical limiting factor, restricting duration of observation sessions.

Similar considerations are true also for each rotation position in a regular observation session, except that these positions contain much less number of frames and represent shorter time intervals. Assuming, that nature of changes in relative orientation of subsystems remain generally independent of rotation, the same linear drift model can be applied to whole duration of a regular session.

Example of results for a regular observation session is presented on Figure 7. Two full rotations were made with ~70 dg step, taking 12 frames in each position. Resulting corrected ellipsoidal zenith positions are plotted in CCD coordinate system (view from below). Consecutive rotation positions are connected by lines. Linear drift in relative subsystem orientation is estimated to be ~5″/h, rendering the ideally circular trajectory of zenith positions (red circle) into a semblance of spiral (green). As time and angle intervals between rotation positions are not precisely equal, actual trajectory does not lay exactly on a regular spiral. Projection of vertical deflection on topocentric coordinate system is represented by the radius (red line), pointing to the position on circle, where CCD Y-axis was oriented to South; direction of topocentric coordinate axes for this moment are shown in the center of circle.

Parameters of data model, approximating observation session results, are calculated using a least squares algorithm. Approximation residuals for each frame are shown on Figure 7 as lines, connecting frame positions to corresponding calculated positions on model trajectory, representing frame time moment and orientation azimuth. Model residual rms for such session is generally a little bigger than for a single static position of similar duration, probably due to some effects, unaccounted for in the model. Also, rotation and re-leveling of instrument might cause some mechanical deviations in instrument assembly. Residuals for individual rotation positions tend to show noticeable systematic component, indicating presence of unaccounted quasi-incidental influences with periods within a few minutes to tens of minutes range and amplitude of up to several tenths of arc second. The

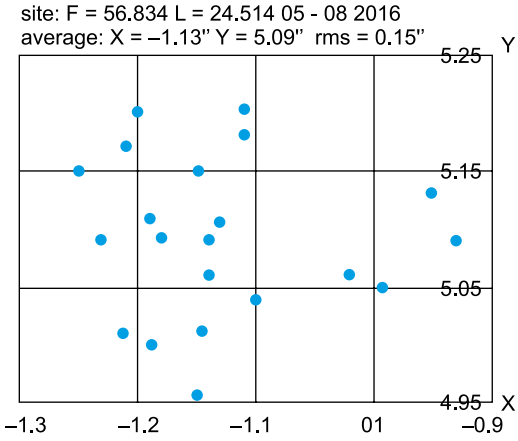

Fig. 8. Vertical deflection values in the test site (May–August 2016), in arc seconds. Each point is result of one observation session, consisting of 100–200 frames in 10–20 positions

most probable candidates are variability of refraction properties in atmosphere and small mechanical deformations in instrument assembly, presumably of thermal origin. Further investigation should provide more knowledge of these effects.

Results of vertical deflection value determination in the test site, are presented on Figure 8, as components of angle between plumb line and reference ellipsoid's normal, in arc seconds. Component Y is in S–N direction (same as component ξ in e.g. (Torge 2001) – positive if plumb line is to the North from ellipsoidal zenith); X– in W–E direction (same as η – positive if plumb line is to the East from ellipsoidal zenith). The process of adjustment of some hardware and software components was still continuing, so consistency of these results may be somewhat compromised and dispersion – a bit overestimated. Besides, due to location of the test site in proximity of sea (35 km) and a large river (1 km), some anomalous refraction effects are suspected.

In order to test the instrument in real field conditions, 6 observation sessions in different locations were performed. The properties of results were similar to the test site. One of locations was selected because of well-known astronomical longitude that could be used for external test of the instrument – the site of former Time Service transit instrument in Riga. Although observation conditions there are not perfect due to city lights and proximity of city transport, resulting in high level of microseismics (with amplitude up to several arc seconds), the result was close to value, calculated as difference of astronomical and geodetical longitudes (diverged from it by 0.1″).

In general, test results show similar accuracy properties as reported for other digital zenith cameras (Hirt 2004; Hirt, Seeber 2008; Tian *et al.* 2014). Now our intention is to proceed with field observations in various sites. Also, some improvements in instrument construction, accessories and control software are planned.

References

Abele, M.; Balodis, J.; Janpaule, I.; Lasmane, I.; Rubans, A.; Zariņš, A. 2012. Digital zenith camera for vertical deflection determination, *Geodesy and Cartography* 38: 123–129. https://doi.org/10.3846/20296991.2012.755324

Hirt, C. 2004. *Entwicklung und Erprobung eines digitalen Zenitkamerasystems für die hochpräzise Lotabweichungsbestimmung*: Doktor- Enginier. Wissenschaftliche Arbeiten der Fachrichtung Vermessungswesen der Universität Hannover. 207 p. [online], [cited 28 November 2016]. Available from Internet: http://www.gbv.de/dms/goettingen/395931258.pdf

Hirt, C.; Bürki, B.; Somieski, A.; Seeber, G. 2010. Modern determination of vertical deflections using digital zenith cameras, *Journal of Surveying Engineering* 136(1): 1–12. https://doi.org/10.1061/(ASCE)SU.1943-5428.0000009

Hirt, C.; Seeber, G. 2008. Accuracy analysis of vertical deflection data observed with the Hannover Digital Zenith Camera System TZK2-D, *Journal of Geodesy* 82(6): 347–356. https://doi.org/10.1007/s00190-007-0184-7

Kahlmann, T.; Hirt, C.; Ingensand, H. 2004. Hochpräzise Neigungsmessung mit dem elektronischen Einachspendelsystem HRTM, in *14th International Conference on Engineering Surveying*, 15–19 März 2004, Zürich [online], [cited 28 November 2016]. Available from Internet: http://www.geometh-data.ethz.ch/downloads/Kahlmann_HRTM_IV2004.pdf

Tian, L.; Guo, J.; Han, Y., *et al.* 2014. Digital zenith telescope prototype of China, *Chinese Science Bulletin* 59: 1978–1983. https://doi.org/10.1007/s11434-014-0256-z

Torge, W. 2001. *Geodesy*. 3rd ed. Berlin, New York: W. de Gruyter. 432 p. https://doi.org/10.1515/9783110879957

Zariņš, A.; Janpaule, I.; Kaminskis, J. 2014. On reference star recognition and identification, *Geodesy and Cartography* 40: 143–147. https://doi.org/10.3846/20296991.2014.987456

Ansis ZARIŅŠ. Senior researcher at the Institute of Geodesy and Geoinformatics, University of Latvia (Dr. phys. 1988). Research interests: control and data processing systems for satellite observation and astrometric instruments.

Augusts RUBANS. Researcher at the Institute of Geodesy and Geoinformatics, University of Latvia (Mg. sc. phys. 1993). Research interests: design of astrometric equipment, SLR, GNSS.

Gunārs SILABRIEDIS. Director and senior researcher at the Institute of Geodesy and Geoinformatics, University of Latvia (Dr. sc. ing. 2013). Research interests: GNSS network analysis, height systems, regional geoid model determination.